Processing and Application of Ceramics 15 [1] (2021) 40–46
https://doi.org/10.2298/PAC2101040S

Molten salt synthesis of TiB_2 nanopowder by reduction of TiO_2 with MgB_2

Liaqat Ali Shah*

State Key Laboratory of Multiphase Complex Systems, Institute of Process Engineering, Chinese Academy of Sciences, Beijing, China

Received 7 July 2020; Received in revised form 8 December 2020; Accepted 11 January 2021

Abstract

This research work presents the preparation of TiB_2 nanopowders by molten-salt synthesis (MSS) technique from TiO_2 and MgB_2 as starting active materials and $MgCl_2$ as a molten salt. The pure TiB_2 nanopowders were finally prepared using 2 M HCl aqueous solution to leach the synthesized samples. The effects of the firing temperature, firing time and reactants to salt ratio on the TiB_2 nanopowders formation were examined. The results demonstrated that the TiB_2 formation was completed even with reactants to salt mass ratio of 1:2 at 1000 °C for 4 h. The TiB_2 nanopowders synthesized with 1:2, 1:5 and 1:10 reactants to salt mass ratios have different particle sizes. Thus, the average particle sizes estimated from BET surface areas were 59, 55 and 46 nm for the samples synthesized with 1:2, 1:5 and 1:10 reactants to salts mass ratios, respectively. These results illustrated that the high concentration of $MgCl_2$ plays a key role in the particles' size reduction. The above results assured that this research study presents a new low-temperature synthesis route for nano-sized metal diboride powders.

Keywords: *molten salt synthesis, low temperature, surface area, TiB_2, particle size*

I. Introduction

Titanium diboride (TiB_2) is an important ultra-high temperature ceramic material possessing a sole combination of exceptional properties which makes it a suitable candidate for a variety of high temperature technological applications. Thus, it can be used as: high temperature wear-resistant material, electrode in metal smelting-cells, surface protection material in impact resistant armours, refractories for molten-metal contact, cutting tools, shielding material in reactor for nuclear fusion etc. [1–3]. The attractive properties which recommend TiB_2 as a promising and attractive material for a different variety of applications are: high hardness (33 GPa), elastic modulus (~560 GPa), melting point (3225 °C), relatively low density (4.52 g/cm^3), good thermal (60–120 W m^{-1} K^{-1}) and electrical (~7.6×10^6 S/m) conductivities and excellent corrosion resistance [1,4–6]. The metal borides synthesis is known for over 100 years, however, to develop inexpensive methods for high yielding quality final products with remarkable properties and applications remains an experimental challenge. So far, several techniques have been reported to prepare metal diborides powders including mechanical alloying [7–9], carbothermal reduction [10,11], boro/carbothermal reduction [11–15], borocarbide reduction [16,17], direct elemental reaction by "self-propagating high temperature synthesis (SHS)" [18,19], sol-gel method [20,21], molten salt electrolysis [22], chemical synthesis routs [23,24], aluminium melt reaction [25], metallothermic reduction via HEBM [8,26,27] and volume combustion process [28]. Unfortunately, these conventional techniques have one of the following disadvantages: requirement of special reaction vessels, high processing temperature and long time, expensive/flammable and/or toxic raw materials as initial reactants (e.g. elemental B, Ti, Mg and $NaBH_4$), and contamination from milling-media caused by prolonged milling. In this regard, the chemists, engineers and material scientists are still experimenting to find an effective and optimal method for metal diboride synthesis.

In addition to conventional techniques for the metal diborides synthesis, a novel molten-salt synthesis

* Corresponding authors: tel: +86 13263353213,
e-mail: *liaqat@uop.edu.pk, drliaqatphy@yahoo.com*

(MSS) technique has recently been developed. In this procedure, high contents of salt are added to the initial reactants mixture which melts during heating above their melting point and works as a reaction media to produce a pool of anion and cations. This reaction medium plays a vital role to expedite the mass transport via convection/diffusion and thus lower the reaction temperature. Moreover, the MSS process has the following several advantages: high phase and chemical purity, low synthesis temperature, exceptional control of particle-morphology, narrow size distribution of crystallites and low aggregation levels in the resultant products, large-scale production, minimal energy consumption and low-cost. Thanks to MSS technique, CeB_6, CaB_6, HfB_2 and NbB_2 have been synthesized in a LiCl/KCl salt at relatively low temperatures [29]. However, flammable Mg and expansive hazardous $NaBH_4$ components were used as reducing agents and B source, respectively. Wei *et al.* [30] and Ran *et al.* [31] synthesized TaB_2 and NbB_2 nanopowders, respectively, via borothermic reduction in NaCl/KCl salt mixture, but they also used expensive elemental B powder. Zhang *et al.* [32] and Bao *et al.* [33] synthesized ZrB_2 and TiB_2 powders, respectively, by a molten salt-assisted magnesio-thermic reduction technique from relatively cheap raw materials, however, they still used the flammable elemental Mg and also the yield of the finally obtained product was very low. Nevertheless, to our knowledge, no work on the TiB_2 preparation from relatively cheap and environmentally friendly materials mixture (i.e. TiO_2 and MgB_2) in molten salt has been reported to date.

In the present research work, the molten-salt assisted magnesio/borothermic reduction technique was developed to synthesize high-quality TiB_2 fine powder at relatively low temperature, from fairly cheap titanium, magnesium and boron source raw materials. The influences of salt concentration, synthesis temperature and firing time on the powder formation of metal diboride were examined with the aim to optimize the synthesis conditions.

II. Experimental details

TiB_2 nanopowders were prepared by the molten-salt synthesis (MSS) technique, and the corresponding flowchart is presented in Fig. 1. Commercial TiO_2 (purity ≥99.98%, Sinopharm Chemical Reagent Co. Ltd. China) and MgB_2 (purity ≥99.9%, Puyang Ruichi New Material Technology Co. Ltd. China) powders were selected as the starting reactants. Anhydrous $MgCl_2$ (≥99.97% purity, Sigma Aldrich) was used to build-up a molten-salt medium.

In the MSS process, the molar ratio of TiO_2/MgB_2 was taken as 1:1.25, as estimated from the stoichiometric composition of reaction 1:

$$TiO_2 + \frac{5}{4}MgB_2 \longrightarrow TiB_2 + \frac{5}{4}MgO + \frac{1}{4}B_2O_3 \quad (1)$$

The reactants were mixed and ground by hand using mortar and pestle. The ground reactants powders were further combined with $MgCl_2$. The mass ratios for initial reactants to salt were 1:0, 1:2, 1:5 and 1:10. The resultant powder mixtures were put into the alumina crucible and covered with a lid. The crucible was then placed in the horizontal alumina-tube furnace and heated under the flowing argon gas with a heating rate of 10 °C/min. The powder mixtures were heated at 800, 900 and 1000 °C for different times before cooling the furnace to ambient temperature.

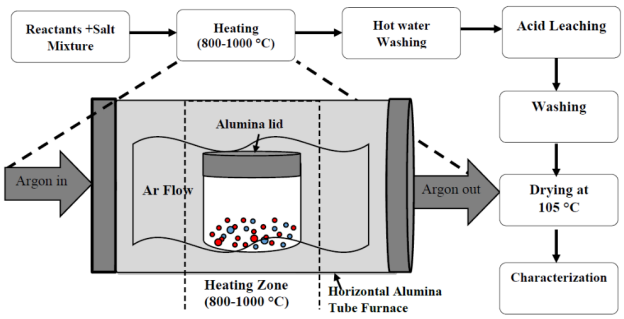

Figure 1. Flowchart of the MSS technique

The product obtained from metal oxide and MgB_2 mixture after heating was washed frequently with hot deionized-water to eliminate the salt contents. The product was further leached with 2 M HCl aqueous solution for 2 h at 80 °C to remove the expected by-products MgO, $Mg_2B_2O_5$ and/or $Mg_3B_2O_6$. Finally, the acid treated powders were collected by centrifugation and washed with deionized water till the removal of Cl^- contents before drying overnight at 105 °C.

Analyses of possible chemical reactions and equilibrium software (HSC Chemistry 6) were applied to get the thermodynamic data including Gibbs free energy and enthalpy values. The qualitative phase analyses of the as-synthesized powders were carried out via X-ray diffraction techniques (XRD, PANalytical, XPERT-PRO MPD). XRD results were recorded at 40 kV and 40 mA using CuKα radiation (λ = 1.5418 Å). For the microstructure observation, the powders were fixed on the alumina stub by an adhesive carbon tape and coated with a thin film of platinum and the micrograph was obtained through a scanning electron-microscope (SEM, JSM-7001F). The energy-dispersive X-ray spectroscopy (EDS) linked with the SEM was used to qualitatively determine the elemental compositions of the synthesized samples. The microstructure and morphology of the synthesized samples were further investigated by TEM (JEM2100, JEOL, Tokyo, Japan) at an accelerating voltage of 200 kV. To set the sample for TEM, the powders were firstly well dispersed in ethanol media under the sonication process, pipetted on to a Cu grid and dried at room temperature. BET surface area measurement was carried out on an AUTOSORB-1 analyser (Quantachrome) by N_2 adsorption-desorption. The equivalent average particle size (d_{BET}) of synthesized

metal diboride powder was estimated from BET surface area (S_{BET}) and the theoretical density of TiB_2 (ρ) according to the following formula $d_{BET} = 6/(S_{BET} \cdot \rho)$. This equation assumes that the particles have a spherical shape with uniform size and low surface roughness [34].

III. Results and discussion

3.1. Influence of firing temperature

Figure 2 shows the influence of firing temperature at constant time of 4 h on the TiB_2 formation from stoichiometric composition (reaction 1) in $MgCl_2$ (initial reactants powder to salt ratio was 1:2). The sample synthesized at 800 °C contains MgO and TiB_2 along with unwanted Mg_2TiO_4 and $Mg_2B_2O_5$ phases (Fig. 2a). These results and thermodynamic data (Fig. 3) indicate that some quantity of TiO_2 is reduced to Ti and MgO by MgB_2. In this reaction the elemental amorphous boron

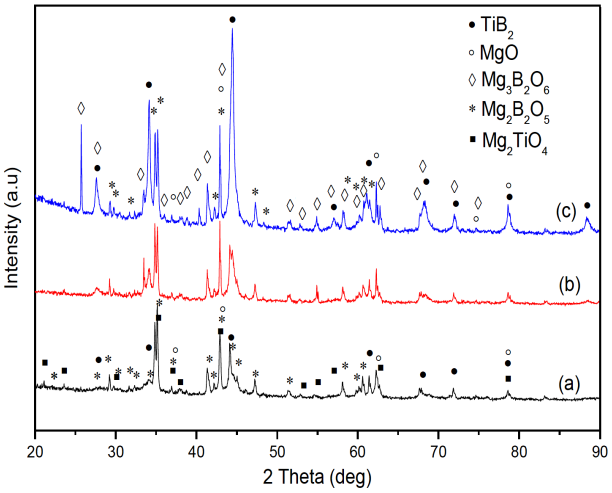

Figure 2. XRD spectra of samples synthesized with stoichiometric composition at: a) 800 °C, b) 900 °C and c) 1000 °C using reactants to salts mass ratio of 1:2

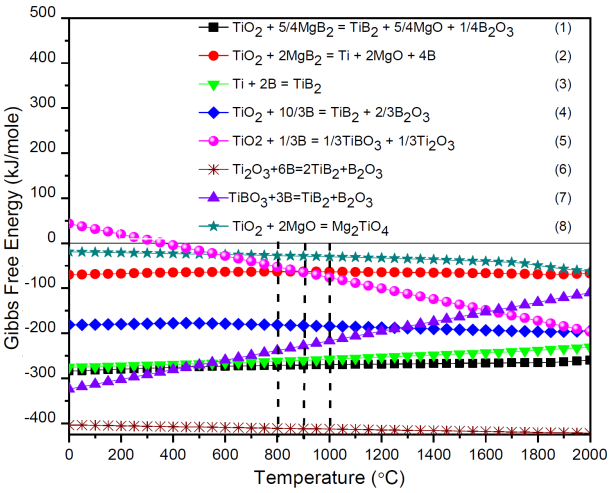

Figure 3. Relationship between the Gibbs free energy and temperature

may also be produced according to reaction 2:

$$TiO_2 + 2\,MgB_2 \longrightarrow Ti + 2\,MgO + 4\,B \qquad (2)$$

Subsequently, the generated B reacted with by-product Ti and un-reacted TiO_2 to form TiB_2 according to following reactions 3 and 4:

$$Ti + 2\,B \longrightarrow TiB_2 \qquad (3)$$

$$TiO_2 + \frac{10}{3}\,B \longrightarrow TiB_2 + \frac{2}{3}\,B_2O_3 \qquad (4)$$

The thermodynamic calculations show that the Gibbs free-energy corresponding to the reaction 3 is more negative than for the reaction 4 in the temperature range used for synthesis (Fig. 3), revealing that the reaction 3 occurs more easily than the reaction 4. The results indicate that the reaction 4 is just initiated, but still not completed. Actually, the reaction 4 can be divided into the following reactions:

$$TiO_2 + \frac{1}{3}\,B \longrightarrow \frac{1}{3}\,TiBO_3 + \frac{1}{3}\,Ti_2O_3 \qquad (5)$$

$$Ti_2O_3 + 6\,B \longrightarrow 2\,TiB_2 + B_2O_3 \qquad (6)$$

$$TiBO_3 + 3\,B \longrightarrow TiB_2 + B_2O_3 \qquad (7)$$

It is understandable that the reactions 6 and 7 occur more easily as they have highly negative Gibbs free energy, however, the reaction 5, which produces the intermediate products Ti_2O_3 and $TiBO_3$, has only moderately negative energy and thus it is not completed at temperature as low as 800 °C. At this temperature, the free energy of the reaction 5 is comparable to the following reaction 8:

$$TiO_2 + 2\,MgO \longrightarrow Mg_2TiO_4 \qquad (8)$$

Therefore, the reaction between un-reacted TiO_2 and by-product MgO occurrs to form Mg_2TiO_4.

$Mg_2B_2O_5$ formation as detected by XRD may be the consequence of the reaction between by-products MgO (from the reaction 2) and B_2O_3 (from the reaction 3) according to the reaction 9:

$$2\,MgO + B_2O_3 \longrightarrow Mg_2B_2O_5 \qquad (9)$$

Upon increasing the synthesis temperature to 900 °C, similar XRD pattern (Fig. 2b) with four phases was observed as for the sample synthesized at 800 °C (Fig. 2a). However, in this case the amount of Mg_2TiO_4 decreased and TiB_2 phase increased. When the firing temperature was increased to 1000 °C (Fig. 2c), the desired TiB_2 phase appeared as a dominant phase, while Mg_2TiO_4 phase disappeared and a new phase of $Mg_3B_2O_6$ was detected, indicating the completion of the TiB_2 formation reaction. The decreasing and finally disappearing of the Mg_2TiO_4 phase with the temperature increase indicate that the sample synthesized at low-temperature also has amorphous boron which was not detected by the XRD.

Thus, with the temperature increase the chances of the reaction 5 occurrence increases and it is finally completed at 1000 °C.

The appearance of $Mg_3B_2O_6$ phase indicates that the expected by-products MgO and B_2O_3 were also reacting together according to the reaction 10:

$$3\,MgO + B_2O_3 \longrightarrow Mg_3B_2O_6 \qquad (10)$$

The overall reaction 1 can be obtained by merging the above intermediate reactions when 1:1.25 molar ratio for TiO_2 and MgB_2 is used.

3.2. *Influence of salt concentration*

Figure 4 shows the XRD results for the samples prepared at temperature 1000 °C with reactants to salt mass ratios of 1:0, 1: 2, 1:5 and 1:10. The patterns indicate that a sample with 1:0 mass ratio has only minor content of TiB_2 phase beside the major phases of Mg_2TiO_4 and MgO (Fig. 4a). When the sample was synthesized in molten salt (i.e. $MgCl_2$) with 1:2 mass ratio, the major phase of desired TiB_2 along with magnesium borates and MgO contents were detected, whereas the intermediate phase of Mg_2TiO_4 disappeared (Fig. 4b). When the ratio of reactants to $MgCl_2$ was decreased to 1:5, no significant changes in the pattern were detected. However, the orientation of $Mg_3B_2O_6$ was changed as it showed an extra peak at $2\theta \approx 21.08°$ and the peak corresponding to $2\theta \approx 25.72°$ was reduced significantly (Fig. 4c). When the salt ratio was further decreased to 1:10, the same shape of XRD pattern was observed as for the sample with 1:5 mass ratio (Fig. 4d), indicating that the high amount of salt contents has the same role in the completion of TiB_2 formation reaction as the sample synthesized at 1000 °C with low salt contents. These results dictated that the low contents of $MgCl_2$ are sufficient to complete the TiB_2 formation reaction. It is well-known that high concentrations of salt at high temperature also contaminate the furnace tube thanks to its high vapour pressure. Thus, the low content of $MgCl_2$ in initial powder could be beneficial for the completion of TiB_2 powder formation reaction but also to avoid the furnace tube contamination.

3.3. *Influence of the firing time*

The XRD patterns of the samples after heating in salt at 1000 °C for 1, 2 and 4 h are shown in Fig. 5. In the sample heated at 1000 °C for 1 h, beside the TiB_2 phase, the phases of MgO, $Mg_3B_2O_6$ and $Mg_2B_2O_5$ were also detected (Fig. 5a). Upon increasing the time to 2 h, the MgO, $Mg_3B_2O_6$ and $Mg_2B_2O_5$ peaks were still detected, however, the peak of TiB_2 increased comparatively (Fig. 5b). When the sample firing time increased to 4 h, the TiB_2 phase was increased further and appeared as a dominant phase (Fig. 5c).

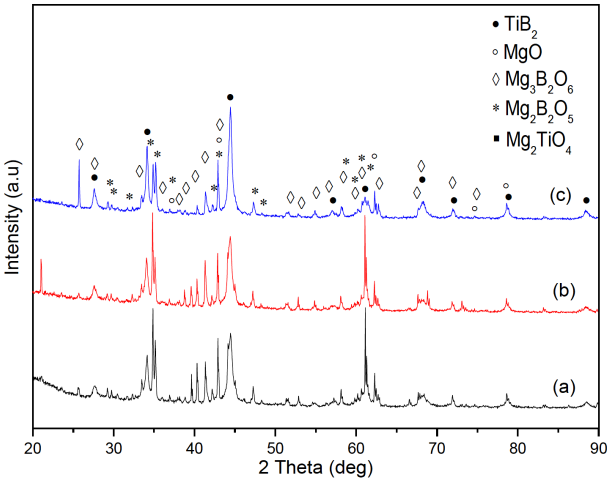

Figure 5. XRD results for samples prepared at 1000 °C for: a) 1 h, b) 2 h and c) 4 h, with reactants to salt mass ratio of 1:2

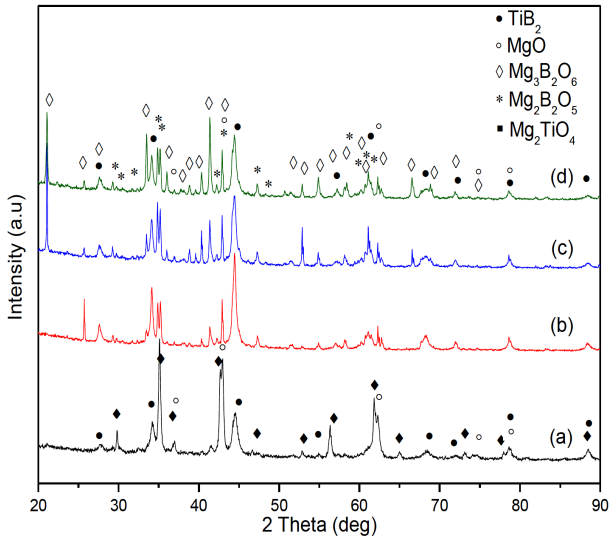

Figure 4. XRD results for samples prepared at 1000 °C with reactants to salt mass ratio of: a) 1:0, b) 1:2, c) 1:5 and d) 1:10

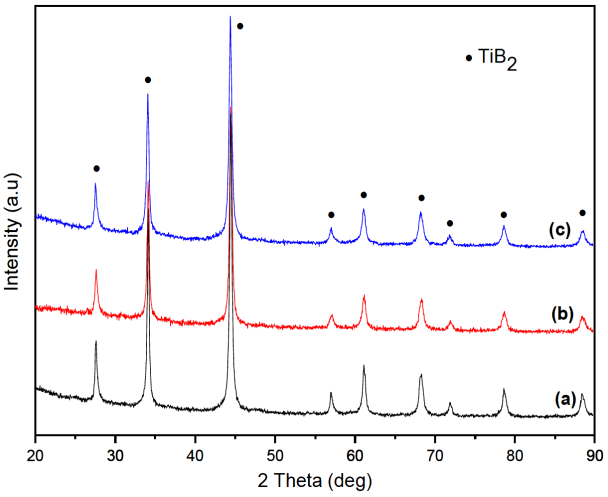

Figure 6. XRD results of samples prepared at 1000 °C with mass ratio for reactants powder to salt of: a) 1:2, b) 1:5 and c) 1:10 after acid leaching

3.4. Influence of acid leaching

XRD patterns of acid leached samples are shown in Fig. 6. After HCl leaching, the sample synthesized at 1000 °C for 4 h with reactants to salt mass ratios of 1:2, 1:5 and 1:10 have almost the same XRD pattern. All the unwanted phases of MgO, $Mg_3B_2O_6$ and $Mg_2B_2O_5$ disappeared and the single phase TiB_2 samples were obtained.

3.5. Microstructural analyses

The SEM results indicate that the TiB_2 powders obtained after 4 h heating in $MgCl_2$ salt at 1000 °C followed by HCl leaching and washing consist of nano-sized particles (Fig. 7). The particle size and shape of the product materials are quite different from the initial raw material TiO_2 (Fig. 7a) indicating the dominance of "dissolution-precipitation" mechanism during the TiB_2 formation. The particle/grain sizes, estimated from micrographs by nano-measurer are mostly smaller than 100 nm having decreasing tendency with the decrease of reactants to salt mass ratio. Thus, the average particle size is 250, 150 and 100 nm for the samples synthesized with mass ratios 1:2, 1:5 and 1:10, respectively. The TEM images further confirmed the nano-sized nature of the prepared TiB_2 particles (Fig. 8).

The EDS spectra (Fig. 7i-k) show mainly the presence of Ti and B in the entire leached sample confirming the formation of pure TiB_2 nano-powder which is in good agreement with the XRD results (Fig. 6). This could imply that the reaction is completed at 1000 °C even with reactants to salt mass ratio of 1:2. The higher concentration of salt played a central role in the particle size reduction which is also one of the dire needs of the day for TiB_2 use in industrial sector. The related EDS analysis detected negligible contents of Mg and small amount of O, which is a clear proof of the removal of

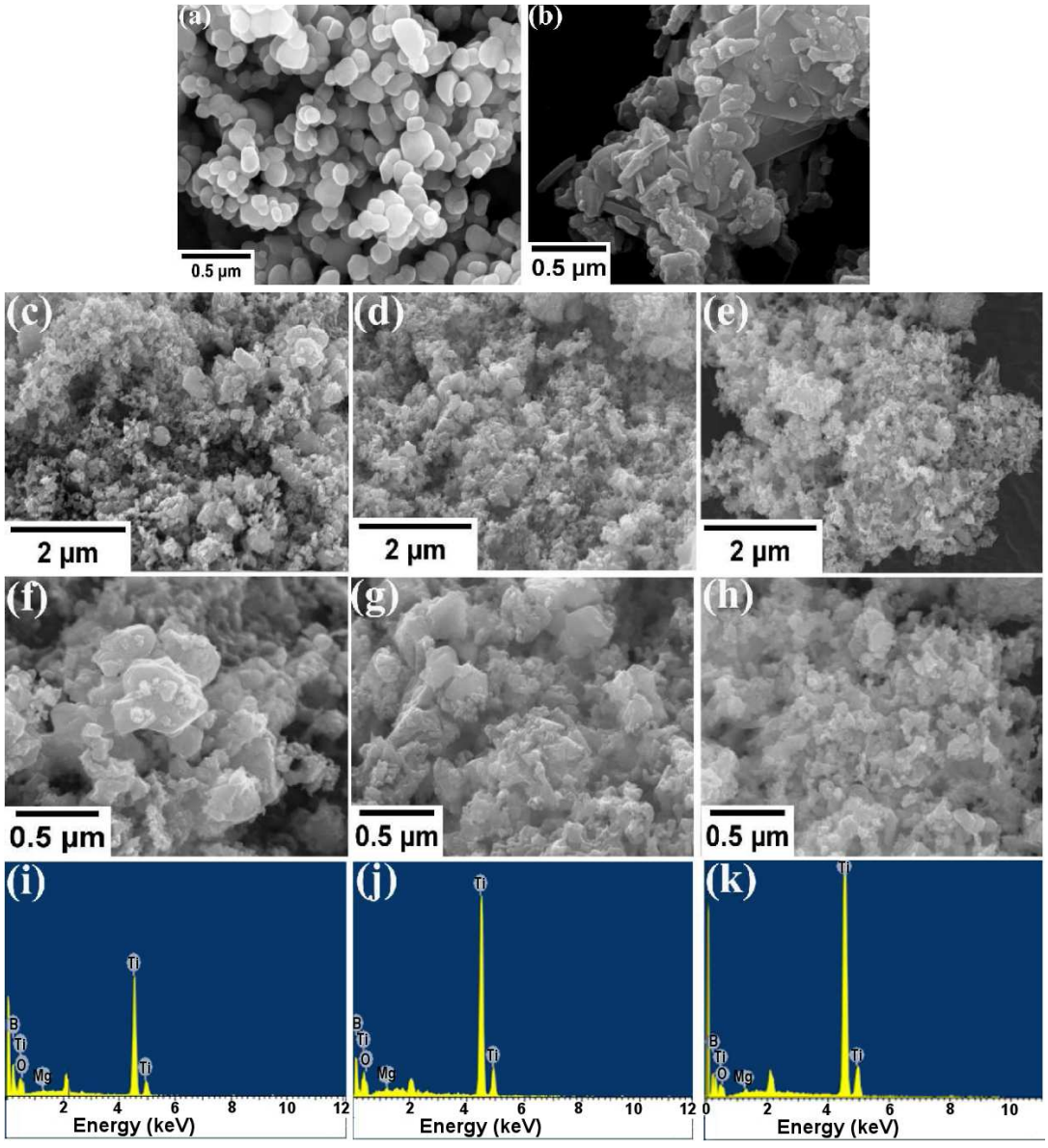

Figure 7. SEM micrograph of initial reactants: a) TiO_2 and b) MgB_2, and SEM images with EDS of samples prepared with reactants to salt mass ratios of 1:2 (c, f, i), 1:5 (d, g, j) and 1:10 (e, h, k), heated at 1000 °C for 4 h and leached with HCl

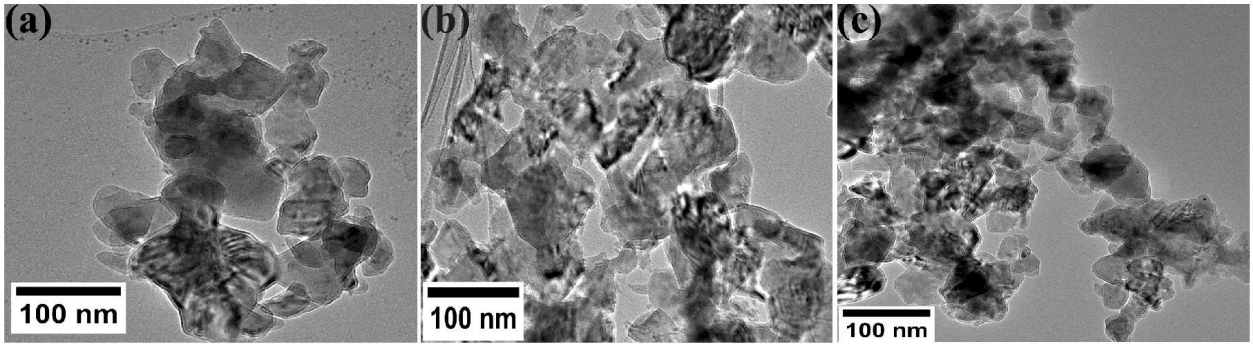

Figure 8. TEM images of acid leached samples synthesized with reactants to salt mass ratios of: a) 1:2, b) 1:5 and c) 1:10 and heated at 1000 °C for 4 h

Table 1. Specific surface area S_{BET} and equivalent average particle size d_{BET} of the synthesized TiB_2 nanopowders

Reactants to salt mass-ratio	S_{BET} [m^2/g]	d_{BET} [nm]
1:2	22	59
1:5	24	55
1:10	28	46

MgO and $Mg_3B_2O_6$ compounds after acid leaching. The presence of oxygen in the synthesized samples could be due to samples handling in non-inert atmospheric laboratory conditions as already reported in the literature [30,35]. The observed unlabelled peaks are from platinum coating and carbon tape used for SEM.

The product yield was determined based on TiB_2 product amount obtained after acid leaching process and the theoretical amount of TiB_2 as estimated from reaction 1. The calculated value of ≥82 wt.% indicates loss of ≤18 wt.%, which is probably due to the repeated washing with distilled water, filtration, acid (HCl) leaching and centrifugation.

The S_{BET} and the corresponding d_{BET} of the synthesized TiB_2 samples are tabulated in Table 1. These results revealed that the S_{BET} and the corresponding d_{BET} of the TiB_2 nanopowders, synthesized with the mass ratio of 1:2 for initial reactant to salt, were 22 m^2/g and 59 nm, respectively. The d_{BET} of the sample synthesized by the MSS technique is much lower than the reported results [8,13,14]. This can be clarified by one or both of the following two reasons: first, the low temperature synthesis played a key role to restrict the growth size of TiB_2 particle; second, the $MgCl_2$ used as a molten-salt can provide a well suited liquid environment during the synthesis to expedite the mass transfer proportion of the initial reactants and constrain the particle growth of the desired product [30,32,35]. After decreasing the reactants to salt mass ratio to 1:5 and 1:10, the S_{BET} of the synthesized TiB_2 powders increased to 24 and 28 m^2/g, respectively, while the d_{BET} reduced to 55 and 46 nm. The particle-size calculated from BET is in a good agreement with the sizes estimated from SEM and TEM micrograph. The BET and SEM results suggest that the particle-size of the synthesized TiB_2 nanopowders decreases with the decrease of reactants to salt ratio.

IV. Conclusions

TiB_2 nano-powders were successfully synthesized by the MSS technique using TiO_2 and MgB_2 as the starting materials and $MgCl_2$ as a molten-salt. The by-product MgO and magnesium borates in the as-synthesized TiB_2 nanopowders, originated from the reaction of TiO_2 and MgB_2, were removed by leaching process using 2 M HCl aqueous solution. The study of the effects of the firing temperature, firing time and reactants to salt ratio on the TiB_2 nanopowders formation demonstrated that the reaction of TiB_2 formation was completed even with mass ratio of 1:2 for reactants powder to salt at temperature as low as 1000 °C with firing time of 4 h. S_{BET} and d_{BET} of the acid leached TiB_2 nanopowders synthesized with 1:2 mass ratios for initial reactants to salt were 22 m^2/g and 59 nm, respectively. Furthermore, it was observed that the increase in molten salt concentrations in the initial reactants played a key role in the accretion of surface area and reduction of particle size of synthesized powder. The TiB_2 nano-powder synthesized with 1:10 mass ratio for initial reactants to salt showed high value of S_{BET} (28 m^2/g) and smaller value of d_{BET} (46 nm). The synthesized nanopowders exhibited hexagonal-like morphology. The EDS observation of the leached samples revealed the formation of TiB_2 nanopowders with a high purity.

Acknowledgements: The author would like to highly acknowledge the financial support by Chinese Academy of Sciences under President's International Support Initiative (PIFI) for Postdoctoral Researchers No. 2017PE0006.

References

1. B. Basu, G.B. Raju, A.K. Suri, "Processing and properties of monolithic TiB_2 based materials", *Int. Mater. Rev.*, **51** (2006) 352–374.
2. R.G. Munro, "Material properties of titanium diboride", *J. Res. Natl. Inst. Stan.*, **105** (2000) 709–720.
3. M. Jones, A.J. Horlock, P.H. Shipway, D.G. McCartney, J.V. Wood, "A comparison of the abrasive wear behaviour of HVOF sprayed titanium carbide- and titanium boride-based cermet coatings", *Wear*, **251** (2001) 1009–1016.
4. B.K. Basu B, "Overview: High-temperature ceramics", pp.

257–285 in *Advanced Structural Ceramics*, Ed. B.K. Basu, John Wiley & Sons, Hoboken, NJ, 2011.
5. B.T. Golla, A. Mukhopadhyay, B. Basu, "Titanium diboride", pp. 316–360 in *Ultra-High Temperature Ceramics*. Eds. W.G. Fahrenholtz, W.E. Lee, Y. Zhou, John Wiley & Sons, Hoboken, NJ, 2014.
6. R.A. Andrievski, "Superhard materials based on nanostructured high-melting point compounds: achievements and perspectives", *Int. J. Refract. Met. Hard Mater.*, **19** (2001) 447–452.
7. Y. Hwang, J.K. Lee, "Preparation of TiB_2 powders by mechanical alloying", *Mater. Lett.*, **54** (2002) 1–7.
8. B. Nasiri-Tabrizi, T. Adhami, R. Ebrahimi-Kahrizsangi, "Effect of processing parameters on the formation of TiB_2 nanopowder by mechanically induced self-sustaining reaction", *Ceram. Int.*, **40** (2014) 7345–7354.
9. W.M. Tang, Z.X. Zheng, Y.C. Wu, J.M. Wang, J. Lu, J.W. Liu, "Synthesis of TiB_2 nanocrystalline powder by mechanical alloying", *Trans. Nonferrous Met. Soc. China*, **16** (2006) 613–617.
10. S.H. Kang, D.J. Kim, "Synthesis of nano-titanium diboride powders by carbothermal reduction", *J. Eur. Ceram. Soc.*, **27** (2007) 715–718.
11. B. Derin, K. Kurtoglu, F.C. Sahin, O. Yucel, "Thermochemical modeling and experimental studies on the formation of TiB_2 through carbothermic synthesis from TiO_2 and B_2O_3 or B_4C", *Ceram. Int.*, **43** (2017) 10975–10982.
12. B. Shahbahrami, F.G. Fard, A. Sedghi, "The effect of processing parameters in the carbothermal synthesis of titanium diboride powder", *Adv. Powder Technol.*, **23** (2012) 234–238.
13. W.M. Guo, G.J. Zhang, Y. You, S.H. Wu, H.T. Lin, "TiB_2 powders synthesis by borothermal reduction in TiO_2 under vacuum", *J. Am. Ceram. Soc.*, **97** (2014) 1359–1362.
14. C. Subramanian, T.S.R.C. Murthy, A.K. Suri, "Synthesis and consolidation of titanium diboride", *Int. J. Refract. Met. Hard Mater.*, **25** (2007) 345–350.
15. L. Ma, J.C. Yu, X. Guo, B.Y. Xie, H.Y. Gong, Y.J. Zhang, Y.X. Zhai, X.Z. Wu, "Preparation and sintering of ultrafine TiB_2 powders", *Ceram. Int.*, **44** (2018) 4491–4495.
16. Y. You, D.W. Tan, W.M. Guo, S.H. Wu, H.T. Lin, Z. Luo, "TaB_2 powders synthesis by reduction of Ta_2O_5 with B_4C", *Ceram. Int.*, **43** (2017) 897–900.
17. E.Y. Jung, J.H. Kim, S.H. Jung, S.C. Choi, "Synthesis of ZrB_2 powders by carbothermal and borothermal reduction", *J. Alloys Compd.*, **538** (2012) 164–168.
18. D.D. Radev, M. Marinov, "Properties of titanium and zirconium diborides obtained by self-propagated high-temperature synthesis", *J. Alloy Compd.*, **244** (1996) 48–51.
19. A.K. Khanra, L.C. Pathak, S.K. Mishra, M.M. Godkhindi, "Effect of NaCl on the synthesis of TiB_2 powder by a self-propagating high-temperature synthesis technique", *Mater. Lett.*, **58** (2004) 733–738.
20. L. Baca, N. Stelzer, "Adapting of sol-gel process for preparation of TiB_2 powder from low-cost precursors", *J. Eur. Ceram. Soc.*, **28** (2008) 907–911.
21. A. Rabiezadeh, A.M. Hadian, A. Ataie, "Synthesis and sintering of TiB_2 nanoparticles", *Ceram. Int.*, **40** (2014) 15775–15782.
22. V.I. Taranenko, I.V. Zarutskii, V.I. Shapoval, M. Makyta, K. Matiasovsky, "Mechanism of the cathode process in the electrochemical synthesis of TiB_2 in molten-salts. 2. Chloride fluoride electrolytes", *Electrochim. Acta*, **37** (1992) 263–268.
23. L.Y. Chen, Y.L. Gu, Y.T. Qian, L. Shi, Z.H. Yang, J.H. Ma, "A facile one-step route to nanocrystalline TiB_2 powders", *Mater. Res. Bull.*, **39** (2004) 609–613.
24. R.L. Axelbaum, D.P. DuFaux, C.A. Frey, K.F. Kelton, S.A. Lawton, L.J. Rosen, S.M.L. Sastry, "Gas-phase combustion synthesis of titanium boride (TiB_2) nanocrystallites", *J. Mater. Res.*, **11** (1996) 948–954.
25. P.T. Li, Y.Y. Wu, X.F. Liu, "Controlled synthesis of different morphologies of TiB_2 microcrystals by aluminum melt reaction method", *Mater. Res. Bull.*, **48** (2013) 2044–2048.
26. A. Nozari, S. Heshmati-Manesh, A. Ataie, "A facile synthesis of TiB_2 nano-particles via mechano-thermal route", *Int. J. Refract. Met. Hard Mater.*, **33** (2012) 107–112.
27. N.J. Welham, "Formation of nanometric TiB_2 from TiO_2", *J. Am. Ceram. Soc.*, **83** (2000) 1290–1292.
28. A. Nekahi, S. Firoozi, "Effect of KCl, NaCl and $CaCl_2$ mixture on volume combustion synthesis of TiB_2 nanoparticles", *Mater. Res. Bull.*, **46** (2011) 1377–1383.
29. D. Portehault, S. Devi, P. Beaunier, C. Gervais, C. Giordano, C. Sanchez, M. Antonietti, "A general solution route toward metal boride nanocrystals", *Angew. Chem. Int. Edit.*, **50** (2011) 3262–3265.
30. T.T. Wei, Z.T. Liu, D.L. Ren, X.G. Deng, Q.H. Deng, Q. Huang, S.L. Ran, "Low temperature synthesis of TaB_2 nanorods by molten-salt assisted borothermal reduction", *J. Am. Ceram. Soc.*, **101** (2018) 45–49.
31. S.L. Ran, H.F. Sun, Y.N. Wei, D.W. Wang, N.M. Zhou, Q. Huang, "Low-temperature synthesis of nanocrystalline NbB_2 powders by borothermal reduction in molten salt", *J. Am. Ceram. Soc.*, **97** (2014) 3384–3387.
32. S.W. Zhang, M. Khangkhamano, H.J. Zhang, H.A. Yeprem, "Novel synthesis of ZrB_2 powder via molten-salt-mediated magnesiothermic reduction", *J. Am. Ceram. Soc.*, **97** (2014) 1686–1688.
33. K. Bao, Y. Wen, M. Khangkhamano, S.W. Zhang, "Low-temperature preparation of titanium diboride fine powder via magnesiothermic reduction in molten salt", *J. Am. Ceram. Soc.*, **100** (2017) 2266–2272.
34. L. Shi, Y. Gu, L. Chen, Z. Yang, J. Ma, Y. Qian, "A convenient solid-state reaction route to nanocrystalline TiB_2", *Inorg. Chem. Commun.*, **7** (2004) 192–194.
35. D. Liu, Y. Chu, S. Jing, B. Ye, X. Zhou, "Low-temperature synthesis of ultrafine TiB_2 nanopowders by molten-salt assisted borothermal reduction", *J. Am. Ceram. Soc.*, **101** (2018) 5299–5303.